

Knockdown of Transient Receptor Potential Canonical-1 Reduces the Proliferation and Migration of Endothelial Progenitor Cells

Chun-yan Kuang, Yang Yu, Kui Wang, De-hui Qian, Meng-yang Den, and Lan Huang

Endothelial progenitor cells (EPCs) play an important role in accelerating endothelial repair after vascular injury. The proliferation and migration of EPCs is a critical first step in restoring endothelium. However, mechanisms for modulating EPC proliferation and migration are still being elucidated. Our previous study found that transient receptor potential canonical-1 (TRPC1) is involved in regulating store-operated Ca^{2+} entry in EPCs through stromal interaction molecule 1. Therefore, in the present study, we sought to further investigate the regulation of proliferation and migration of EPCs by TRPC1. We found that the silencing of TRPC1 by 2 different RNA interference methods suppressed the proliferation and migration of EPCs. In addition, knockdown of TRPC1 significantly reduced the amplitude of store-operated Ca^{2+} entry and caused arrest of the EPC cell cycle in G1 phase. Analysis of the expression of 84 cell cycle genes by microarray showed that 9 genes were upregulated and 4 were downregulated by >2-fold in EPCs following TRPC1 silencing. The genes with expression changes were *Ak1*, *Brca2*, *Camk2b*, *p21*, *Ddit3*, *Inha*, *Sfn1*, *Mdm2*, *Prm1*, *Bcl2*, *Mki67*, *Pmp22*, and *Ppp2r3a*. Finally, we found that a Schlafen 1-blocking peptide partially reversed the abnormal cell cycle distribution and proliferation induced by TRPC1 knockdown, suggesting that Schlafen 1 is downstream of TRPC1 silencing in regulating EPC proliferation. In summary, these findings provide a new mechanism for modulating the biological properties of EPCs and suggest that TRPC1 may be a new target for inducing vascular repair by EPCs.

Introduction

DAMAGE TO THE INTEGRITY of the vascular endothelium contributes to the progression of atherosclerosis, vascular disease, and restenosis after percutaneous coronary interventions [1,2]. Therefore, restoring the injured endothelium helps to prevent atherosclerosis progression and restenosis. In the past, it was thought that endothelial damage was repaired through the proliferation and migration of neighboring endothelial cells [3]. However, recent evidence indicates that endothelial progenitor cells (EPCs) are mobilized from bone and participate in the process of vascular endothelium repair by replacing dysfunctional endothelial cells after injury [4]. The proliferation and migration of EPCs is a critical first step in restoring the endothelium. However, the exact mechanism of EPC proliferation and migration as part of the re-endothelialization process is still being elucidated.

Changes in intracellular calcium concentration ($[\text{Ca}^{2+}]_i$) regulate cell-signaling processes, including cell proliferation, migration, and death. Store-operated Ca^{2+} entry (SOCE) is a major mechanism for Ca^{2+} entry in non-excitable cells such as EPCs. Store-operated calcium chan-

nels (SOCs), which mediate SOCE, are expressed ubiquitously in all cell types [5]. SOC channels are critical for regulating a variety of cellular functions, including cell growth and differentiation [6]. SOC channels are composed of a stromal interaction molecule (STIM), ORAI and the transient receptor potential canonical (TRPC) family, such as TRPC1. The *TRPC1* gene is found on human chromosome 3 and on mouse chromosome 9 [7]. It has been shown that TRPC1 can mediate the physiological function of a variety of cell types [8]. Recently, researchers discovered that TRPC1 is associated with vascular system function. Paria et al. [9] reported that TRPC1 overexpression in a human dermal microvascular endothelial cell line resulted in marked endothelial barrier dysfunction in response to thrombin. Other evidence demonstrated that TRPC1 plays a role in pulmonary artery smooth muscle cell (SMC) proliferation [10]. Moreover, another study found that an antibody to TRPC1 decreased neointimal hyperplasia after vascular injury by inhibiting SMC proliferation [11]. Because EPCs can reduce neointimal formation after vascular injury, we hypothesize that TRPC1 can regulate the function of EPCs. Previously, we reported that TRPC1 is expressed in EPCs and cooperates

with STIM1 to mediate the SOCE of EPCs [12]. However, the exact role of TRPC1 in EPCs is unclear.

The present study was designed to investigate the role of TRPC1 in the proliferation and migration of EPCs. First, we characterized the expression of TRPC1 in rat bone marrow (BM)-derived EPCs. Second, we investigated whether TRPC1 silencing affects the proliferation and migration of EPCs. Finally, we explored the mechanism by which TRPC1 silencing affects EPC function by analyzing gene expression and identifying genes with altered expression in response to TRPC1 silencing.

Methods

Materials and methods are described in detail in the Supplementary Material (Supplementary Data are available online at www.liebertonline.com/scd).

Isolation and characterization of EPCs

Animal procedures were approved by the Care of Experimental Animals Committee of Daping Hospital (approval reference number A5572-01). The investigation conforms with the *Guide for the Care and Use of Laboratory Animals* published by the U.S. National Institutes of Health (NIH Publication No. 85-23, revised 1996). Culturing and characterization of EPCs were performed as previously described [13]. Briefly, male Sprague-Dawley rats were sacrificed by intraperitoneal injection of an overdose of pentobarbital (>50 mg/kg) [14], and then BM was harvested by flushing the femurs and tibias of rats. BM-derived mononuclear cells were isolated by density-gradient centrifugation (Lymphoprep 1.083). Following purification with 3 washing steps, cells were resuspended in low-glucose Dulbecco's modified Eagle's medium (DMEM) supplemented with 20% fetal calf serum (FCS), 100 IU/mL penicillin, 100 mg/mL streptomycin, and vascular endothelial growth factor (VEGF, 50 ng/mL). Next, the cells were seeded onto cell culture flasks and incubated at 37°C and 5% CO₂. To confirm the phenotype of EPCs, cells were incubated with acLDL-Dil (10 mg/mL) for 4 h, fixed with 4% paraformaldehyde, and then incubated with fluorescein isothiocyanate-labeled lectin (UEA-1, 10 mg/mL) for 1 h and examined under a laser confocal scanning microscope (LSCM; FV-300, Olympus). Dual-stained cells positive for acLDL-Dil and UEA-1 were identified as EPCs. Nearly 91% of adherent cells were positive for both markers. Additionally, fluorescence-activated cell sorting (FACS) was performed using antibodies against rat CD34, CD45, VEGFR-2, CD133, and the corresponding isotype control antibodies.

Cell transduction

TRPC1 siRNA(r) (siRNA-TRPC1), TRPC1 shRNA plasmid (r) (shRNA-TRPC1), control siRNA (siRNA-control), and control shRNA (shRNA-control) were purchased from Santa Cruz. Control siRNAs and shRNAs encoded scrambled sequences that should not lead to the specific degradation of TRPC1 mRNA. Transfection of siRNAs and shRNAs was performed according to the manufacturer's instructions. EPCs were transduced with siRNA-TRPC1, shRNA-TRPC1, siRNA-control, and shRNA-control, respectively, for 48 h

before being used in experiments. Uninfected EPCs were used as a blank control.

Cell proliferation studies

[³H]-thymidine incorporation was used to measure DNA synthesis in EPCs as previously described [15]. EPCs were seeded onto 96-well plates, after serum starvation for 24 h, and then transfected with siRNA-TRPC1, shRNA-TRPC1, siRNA-control, and shRNA-control for 48 h. During the final 6–8 h of the transfection, 1 μCi of [methyl-³H]-thymidine was added to each well for 8 h. Last, incorporated [³H]-thymidine was precipitated with 10% trichloroacetic acid and counted with a liquid scintillation counter. In addition, cell number (6-well plates, 1 × 10⁶ cells/well as a baseline) was counted at 0, 24, 48, and 72 h after transfection. Every count was an average of 3 repeats, and each datum point was counted in triplicate.

Cell cycle analysis by flow cytometry

Cell cycle distribution was analyzed using flow cytometry. Briefly, EPCs were trypsinized, centrifuged at 1,500g for 5 min, washed with PBS, and fixed in 70% ethanol overnight at 4°C. Cells were then washed with PBS and incubated in 0.1% sodium citrate containing 0.05 mg of PI and 100 mg/mL RNase for 30 min at room temperature in the dark. Fluorescence analysis was performed on a FACScan flow cytometer (Beckman). The percentage of cells in different phases of the cell cycle was determined using Cell-FIT software.

Cell migration assay

EPC migration was determined using a modified Boyden-chamber assay. EPCs (2 × 10⁵) at 48 h after transfection in 100 μL serum-free DMEM-L) were placed in the upper chamber. DMEM-L with 20% FCS was added to the lower chamber [12]. After 6 h, cells on top of the 8 μm filters were removed, and the filters were rinsed with PBS. Next, the cells on the bottom were fixed with methanol and stained with hematoxylin. Cells that had migrated were counted under a microscope (Leica). In all cases, 5 random high-power fields were counted per chamber. All groups of experiments were performed in triplicate.

Intracellular free Ca²⁺ measurements

EPCs were loaded with the Ca²⁺ indicator Fluo-3/AM for 30 min at 37°C/5% CO₂. The cells were then washed in Hanks' balanced salt solution to remove unloaded Fluo-3/AM, and loaded cells were continuously incubated at 37°C/5% CO₂ for 30 min to facilitate sufficient Fluo-3/AM hydrolysis. After loading, the Fluo-3/AM fluorescence signal was recorded at an excitation wavelength of 488 nm with a digital imaging system equipped with an LSCM at room temperature. Changes in intracellular Ca²⁺ ([Ca²⁺]_i) levels in individual cells were displayed as fluorescence relative to intensity. The SOC-mediated influx of Ca²⁺ following stimulation with 1 μM thapsigargin was measured, as described elsewhere, following Ca²⁺ addition to a final concentration of 2 mM [16]. Additionally, 5 μM nifedipine was added to the solution before the experiment to block voltage-dependent L-type channel activity. All groups of experiments were performed in triplicate.

Gene array analysis

A Cell Cycle PCR Array (a targeted cDNA array consisting of 84 cell cycle regulatory genes) was used according to the instructions of the manufacturer (SABiosciences). Total cellular RNA from EPCs was extracted using TRIzol reagent. Total RNA was measured spectrophotometrically. Complementary DNA was synthesized using a Super Array RT First Strand Kit according to manufacturer's protocol. Real-time reverse transcription-polymerase chain reaction (RT-PCR) was performed using the SYBR Green PCR Master Mix. Data were analyzed with Excel-based PCR array data analysis software (SABiosciences) [17].

Statistical analysis

All results are expressed as mean \pm SD. SPSS11.0 software was utilized for statistical analysis. Statistical analysis was performed using a 2-tailed *t*-test. Values of $P < 0.05$ were regarded as being statistically significant.

Results

Expression of TRPC1 in EPCs

BM-derived EPCs were cultured in DMEM-L supplemented with 20% FCS. Representative BM-derived EPCs exhibited a cord-like, cluster-like, or tubular-like appearance (Fig. 1A). For further characterization, after 4–7 days in

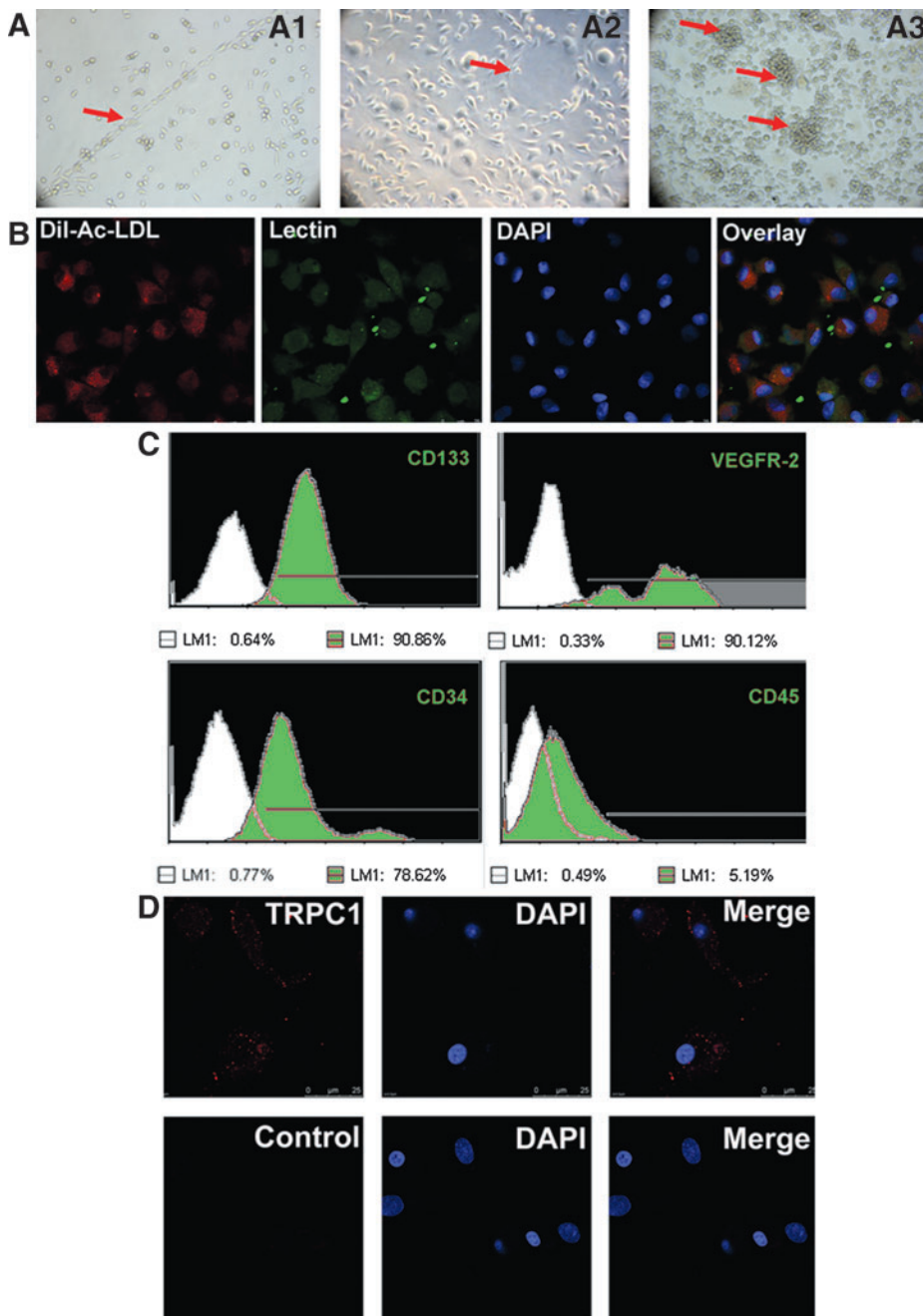


FIG. 1. Characteristics of BM-derived EPCs and localization of TRPC1 in primary EPCs. **(A)** Representative BM-derived EPCs exhibited a cord-like (**A1**), tubular-like (**A2**), or cluster-like (**A3**) appearance (*arrows*). **(B)** EPCs showing uptake of acetylated LDL binding (red) and lectin (green) binding ($90.7\% \pm 1.2\%$, $n=3$; 3 random fields per well). **(C)** Flow cytometry analysis of primary EPCs cultured for 4–7 days. Cells labeled with fluorescent antibodies recognizing CD133, VEGFR-2, CD34, and CD45 are shown as light green areas. The corresponding negative controls are exhibited as the white area on each box, the lines represent a positive gate, and numbers indicate the percentage of positive cells. **(D)** Subcellular localization of TRPC1 in primary EPCs. *Top*: Primary EPCs were incubated with anti-TRPC1 polyclonal antibodies and Cy3-conjugated secondary antibodies. Analysis of the red fluorescent signal (TRPC1) indicates that TRPC1 is predominantly localized to the plasma membrane, with minor staining in the cytoplasm of EPCs. The scale bar represents 25 μ m. *Bottom*: Control EPCs without primary antibody displayed no red fluorescent signal. BM, bone marrow; DAPI, 4, 6-diamidino-2-phenylindole; EPCs, endothelial progenitor cells; TRPC1, transient receptor potential canonical-1; LDL, low-density lipoprotein.

culture (typical culture period before further experiments), attached EPCs were analyzed by a digital imaging system equipped with an LSCM and flow cytometry analysis. LSCM showed that the majority of cells were dual-stained cells ($n > 90.7\%$) positive for both acLDL-DiI and UEA-1 (Fig. 1B). Flow cytometry analysis demonstrated that the cells expressed endothelial stem cell markers, including VEGFR-2, CD34, and CD133, but not CD45 (Fig. 1C).

To investigate TRPC1 expression and subcellular localization in primary EPCs, EPCs were fixed and subjected to immunocytochemistry. As shown in Fig. 1D, TRPC1 was localized predominantly in the plasma membrane but not in intracellular sites in EPCs. Control cells that were not incubated with the antiTRPC1 antibody displayed no red fluorescence. We conclude from these observations that TRPC1 is expressed in primary EPCs and is localized to the plasma membrane.

Suppression of TRPC1 inhibits EPCs proliferation and migration

To evaluate the effects of TRPC1 on EPCs, the proliferation and migration of rat BM-derived EPCs were studied.

First, siRNA-TRPC1, shRNA-TRPC1, siRNA-control, and shRNA-control were transfected into the EPCs. After 48 h of transfection, the transfection efficiency of the control siRNA based on green fluorescence protein expression in cultured EPCs was $89.2\% \pm 1.3\%$ ($n=3$, Supplementary Fig. 1). TRPC1 levels were assessed by real-time RT-PCR and western blotting 48 h post-transduction. Compared with the controls, transfection with siRNA-TRPC1 or shRNA-TRPC1 attenuated TRPC1 expression significantly. TRPC1 mRNA levels were reduced to $38.33\% \pm 0.08\%$ of the control in the siRNA-TRPC1 group and $38.67\% \pm 0.01\%$ in the shRNA-TRPC1 group ($n=3$, $P < 0.05$, Fig. 2A), whereas TRPC1 protein levels were reduced to $38.52\% \pm 2.25\%$ and $39.84\% \pm 1.81\%$, respectively ($n=3$, $P < 0.05$, Fig. 2B). These results indicate that transfection with siRNA-TRPC1 and shRNA-TRPC1 was effective in rat EPCs.

Next, EPC proliferation was analyzed by a [3 H]-thymidine incorporation assay. The results indicated that transfection of EPCs with siRNA-TRPC1 decreased the uptake of [3 H]-thymidine postinfection when compared with the siRNA-control (877.67 ± 13.74 vs. $1,925.67 \pm 24.36$, $n=9$, $P < 0.05$, Fig. 2C). Transfection of EPCs with shRNA-TRPC1 also decreased the uptake of [3 H]-thymidine compared with the shRNA-control (941.00 ± 4.04 vs. $2,058.67 \pm 52.42$, $n=9$, $P < 0.05$, Fig. 2C). At the same time, we performed cell counting to further determine the proliferation of EPCs. Transfection of EPCs with either siRNA-TRPC1 or shRNA-TRPC1 significantly inhibited EPC proliferation compared with the siRNA-control and shRNA-control ($n=3$, $P < 0.05$, Fig. 2D). These results indicate that suppression of TRPC1 inhibits EPC proliferation in vitro.

We also investigated the effects of TRPC1 on EPC migration using the modified Boyden-chamber assay. As shown in Fig. 2E, we observed a notable inhibition of EPC migration in the siRNA-TRPC1 group at 48 h postinfection compared with the siRNA-control (35.29 ± 1.07 vs. 100 ± 2.16 , $n=5$, $P < 0.05$). At the same time, transfection with shRNA-TRPC1 also suppressed the migration of EPCs as compared with the shRNA-control group (39 ± 1.07 vs. 100 ± 2.16 , $n=5$, $P < 0.05$,

Fig. 2E). The above results demonstrate that silencing of TRPC1 suppresses EPC migration in vitro.

Lastly, we measured whether silencing of TRPC1 inhibits SOCE. To activate SOCE, we depleted intracellular Ca^{2+} stores by treating cells with 1 mM thapsigargin in the absence of extracellular Ca^{2+} and then adding extracellular Ca^{2+} to 2 mM. As shown in Fig. 2F, both the siRNA-TRPC1 group and the shRNA-TRPC1 group showed a significant downregulation in SOCE at 48 h after infection compared with the siRNA-control or shRNA-control (siRNA-TRPC1 vs. siRNA-control: 33.88 ± 1.81 vs. 97.33 ± 4.10 ; shRNA-TRPC1 vs. shRNA-control: 27.93 ± 1.60 vs. 101.33 ± 3.28 , $n=6$, $P < 0.05$). These results indicate that SOCE may have an essential role in EPC proliferation and migration.

Taken together, the above data demonstrate that suppression of TRPC1 inhibits EPC proliferation and migration and SOCE in vitro.

Effects of TRPC1 silencing on EPC cell cycle regulation and gene expression

To determine the potential role of TRPC1 silencing on cell cycle regulation in EPCs, the cell cycle distribution was studied using flow cytometry at 48 h after TRPC1 silencing. EPCs were first serum starved for 24 h to obtain synchronization in G_0 , and then transfected with siRNA-TRPC1, shRNA-TRPC1, siRNA-control, and shRNA-control for 48 h. FACS was used to measure the cell cycle distribution. As shown in Fig. 3A and B, $\sim 16.14\%$ of EPCs infected with the siRNA-control progressed into S phase ($n=3$). EPCs infected with siRNA-TRPC1 or shRNA-TRPC1 were distributed mainly in G1 phase. Approximately 2.15% of the siRNA-TRPC1 group and 2.67% of the shRNA-TRPC1 progressed into S phase ($n=3$). These data demonstrate that TRPC1 knockdown causes an arrest in G1 phase of the cell cycle.

To further evaluate the mechanism by which TRPC1 knockdown impacts the cell cycle of EPCs, we analyzed the expression of cell cycle genes using a Cell Cycle PCR gene chips Array. Genes that were either upregulated or downregulated by at least 2-fold in siRNA-TRPC1-infected EPCs compared with the siRNA-control group are listed in Table 1. Of these genes, 9 genes were upregulated in samples from siRNA-TRPC1-infected EPCs as compared with the siRNA-control ($n=3$, $P < 0.05$, Table 1). The upregulated genes were as follows: adenylate kinase 1 (*Ak1*, 3.67-fold), breast cancer 2 (*Brca2*, 2.22-fold), calcium/calmodulin-dependent protein kinase II beta (*Camk2b*, 3.23-fold), cyclin-dependent kinase inhibitor 1A (*p21*, 3.44-fold), DNA-damage inducible transcript 3 (*Ddit3*, 6.96-fold), inhibin alpha (*Inha*, 5.52-fold), Schlafen 1 (*Slfn1*, 9.42-fold), Mdm2 p53 binding protein homolog (*Mdm2*, 2.46-fold), and protamine 1 (*Prm1*, 3.02-fold). Four genes were downregulated in siRNA-TRPC1-infected EPCs compared with the siRNA-control group (Table 1). The downregulated genes were as follows: B-cell CLL/lymphoma 2 (*Bcl2*, 2.72-fold), antigen identified by monoclonal antibody Ki-67 (*Mki67*, 2.24-fold), peripheral myelin protein 22 (*Pmp22*, 2.27-fold), and protein phosphatase 2 (formerly 2A) regulatory subunit B and alpha (*Ppp2r3a*, 2.99-fold). Moreover, the microarray results showed that the gene *Slfn1*, a member of the Schlafen protein family and a negative regulator of cell growth, was upregulated 9.42-fold upon TRPC1 silencing in EPCs.

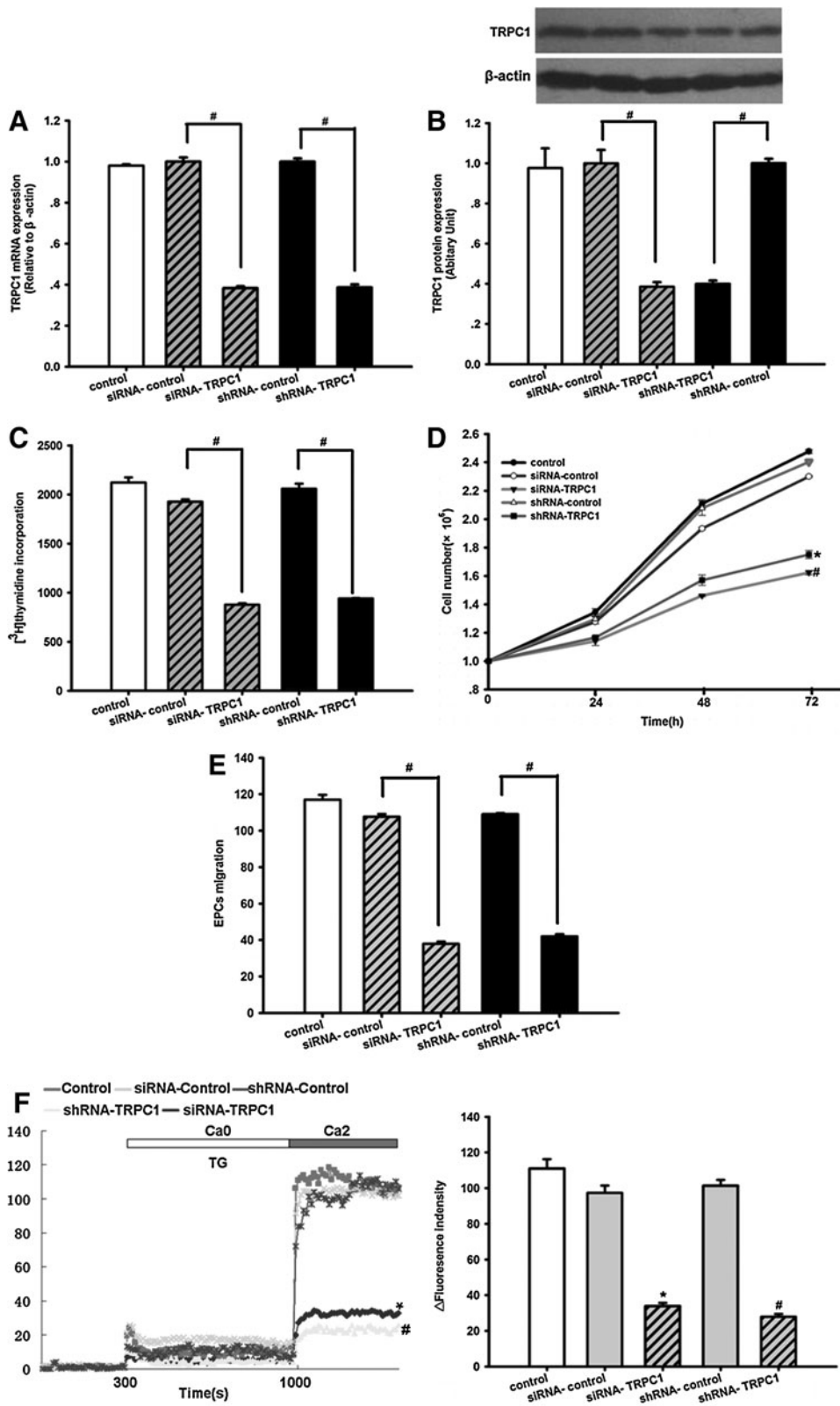


FIG. 2. Silencing of TRPC1 inhibits EPC proliferation and migration. **(A)** TRPC1 mRNA expression levels were determined using real-time RT-PCR. Parallel amplification of the rat housekeeping β -actin gene was used as an internal control. Transduction of EPCs with siRNA targeting TRPC1 (siRNA-TRPC1) or shRNA targeting TRPC1 (shRNA-TRPC1) greatly decreased TRPC1 mRNA expression at 48 h post-transduction. The results are expressed as the mean \pm SEM of 3 experiments. $n=3$, $\#P<0.05$. **(B) Top:** TRPC1 protein levels were examined by western blot analysis. Equal loading was confirmed by staining for β -actin. Transduction of EPCs with siRNA-TRPC1 or shRNA-TRPC1 clearly decreased TRPC1 protein levels at 48 h post-transduction. The data shown are representative of 3 different experiments. *Bottom:* Densitometric analysis of TRPC1 protein expression levels, normalized to expression levels of the housekeeping β -actin gene, was determined using the Quantity One program. The results are expressed as the mean \pm SEM ($n=3$), $\#P<0.05$. **(C)** Effects of TRPC1 knock-down on EPC proliferation. A [3 H]-thymidine incorporation assay was used to examine EPC proliferation. Transfection of EPCs with siRNA-TRPC1 or shRNA-TRPC1 significantly decreased the uptake of [3 H]-thymidine by EPCs at 48 h after infection. The data are presented as the mean \pm SEM ($n=9$), $\#P<0.05$. **(D)** Transfection of EPCs with siRNA-TRPC1 or shRNA-TRPC1 clearly inhibited the proliferation of EPCs at 48 h after infection. The data are presented as the mean \pm SEM ($n=3$), $\#P<0.05$ versus siRNA-control, $*P<0.05$ versus shRNA-control. **(E)** Silencing of TRPC1 inhibited EPC migration, as analyzed by a

modified Boyden-chamber assay. Transfection of EPCs with siRNA-TRPC1 or shRNA-TRPC1 notably decreased the number of migrating EPCs. The data are presented as the mean \pm SEM ($n=5$), $\#P<0.05$. **(F)** The SOC-mediated influx of Ca^{2+} was examined under stimulation with $1 \mu M$ thapsigargin during the change from Ca^{2+} -free conditions to $2 mM$ Ca^{2+} . *Left:* The maximum amplitude of $[Ca^{2+}]_i$ induced by SOCE significantly decreased after transfection with siRNA-TRPC1 or shRNA-TRPC1 for 48 h. *Right:* Statistical analysis of SOCE among different groups. The data are presented as the mean \pm SEM of 3 different experiments, $n=6$, $\#P<0.05$ versus shRNA-control, $*P<0.05$ versus siRNA-control. RT-PCR, reverse transcription-polymerase chain reaction; SEM, standard error mean; SD, standard deviation; SOCs, store-operated calcium channels; SOCE, store-operated Ca^{2+} entry.

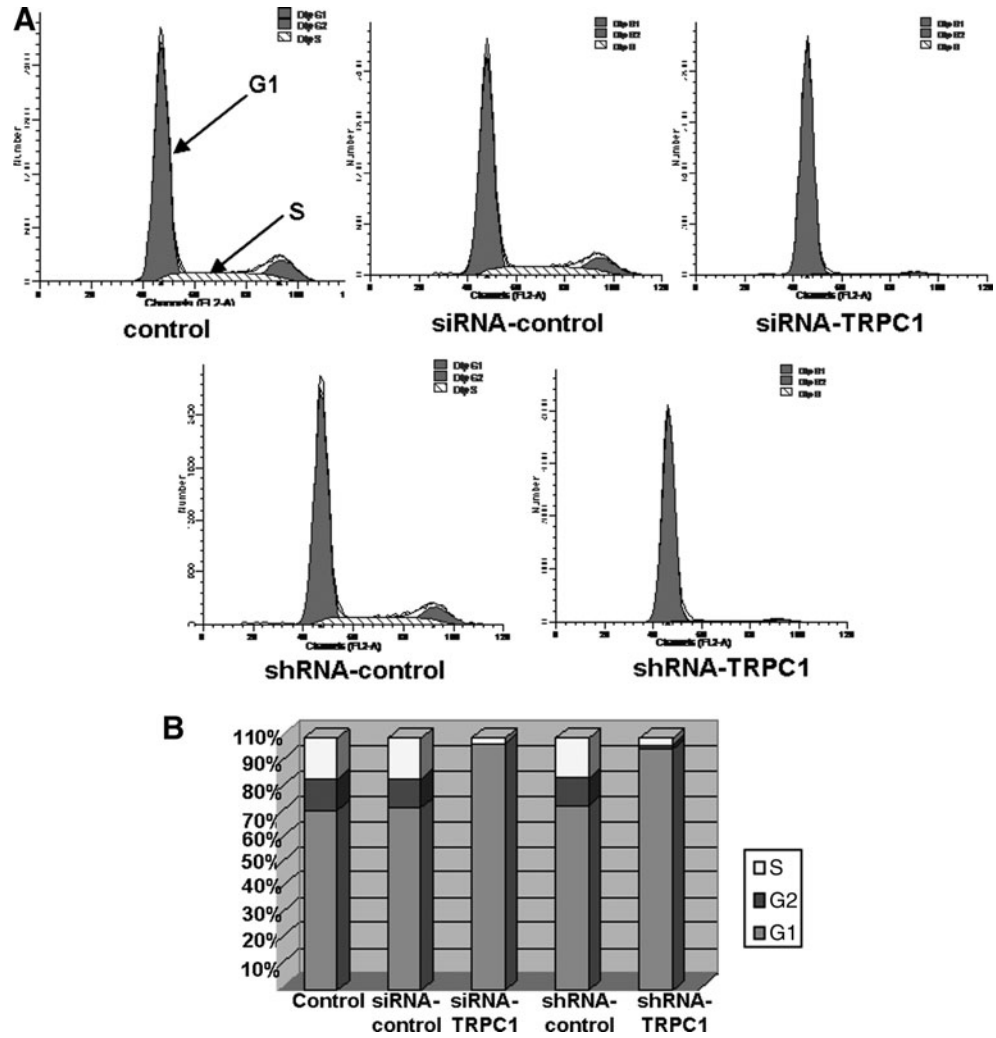


FIG. 3. Effects of TRPC1 knockdown on cell cycle regulation in EPCs. **(A)** Flow cytometry was performed on EPCs transfected with siRNA-TRPC1, shRNA-TRPC1, siRNA-control, and shRNA-control for 48 h. Data shown are a representative pattern of cell cycle distribution in synchrony. **(B)** Average cell cycle distribution data from 3 different experiments, $n=3$.

However, the role of Slfn1 in EPC proliferation and migration remains unknown at present.

Impact of Slfn1 on EPC proliferation following TRPC1 silencing

Slfn1 has been reported to cause arrest in the G1 phase of the cell cycle [18]. To further confirm the increased expression of Slfn1 in response to TRPC1 silencing, we performed real-time RT-PCR and western blot analysis. As shown in Fig. 4A, a 9.1-fold increase in Slfn1 mRNA levels ($n=3$, $P<0.05$) and an 8.6-fold increase in Slfn1 protein levels was detected when compared with the siRNA-control ($n=3$, $P<0.05$, Fig. 4B).

Next, we tested the impact of Slfn1 inhibition combined with TRPC1 silencing on EPC proliferation. To inhibit Slfn1 expression, EPCs were transfected with either siRNA-TRPC1 alone or with siRNA-TRPC1 and an Slfn1-blocking peptide. Interestingly, we found that the G1 arrest induced by TRPC1 silencing was partially reversed in the presence of the Slfn1-blocking peptide. The S-phase population was increased when EPCs is being stimulated in the presence of siRNA-

TRPC1 and the Slfn1-blocking peptide ($n=3$, $P<0.05$, Fig. 4C), whereas the control antibody did not affect the cell cycle distribution. In addition, the proliferation of EPCs under siRNA-TRPC1 and Slfn1-blocking peptide stimulation was partially restored compared with the siRNA-TRPC1 group ($n=3$, $P<0.05$, Fig. 4D). Lastly, the reduced uptake of [³H]-thymidine by EPCs following TRPC1 silencing was also partially reversed by the Slfn1-blocking peptide ($n=9$, $P<0.05$, Fig. 4E). Taken together, these results indicate that Slfn1 acts downstream of TRPC1 silencing in EPCs.

Discussion

The major findings of the present study were as follows: (1) TRPC1 is localized predominantly to the plasma membrane in EPCs; (2) the proliferation and migration of EPCs were inhibited by 2 different TRPC1 silencing methods; (3) SOCE was suppressed by knockdown of TRPC1; (4) upon knockdown of TRPC1 expression, the EPC cell cycle was arrested in G1 phase; additionally, 9 genes were upregulated and 4 genes downregulated at least 2-fold, indicating they may mediate the effects of TRPC1 on EPC proliferation.

These genes were *Ak1*, *Brca2*, *Camk2b*, *p21*, *Ddit3*, *Inha*, *Slfn1*, *Mdm2*, *Prm1*, *Bcl2*, *Mki67*, *Pmp22*, and *Ppp2r3a*, and (5) *Slfn1* functions downstream of TRPC1 silencing in EPCs. An *Slfn1*-blocking peptide partially reversed the cell cycle distribution and proliferation changes induced by TRPC1 knockdown. Taken together, these findings provide a new mechanism for modulating the biological properties of EPCs and suggest that TRPC1 may be a new target for inducing vascular repair by EPCs.

TRPC1, the first identified member of the TRP channel family, was initially discovered in *Drosophila* and was found to be responsible for the visual response of the fly [19]. Ca^{2+} influx through TRPC1 has been demonstrated to be important for regulating cell proliferation, migration, and differentiation [20–22]. In addition, evidence suggests that TRPC1 is a member of the SOCs and modulates Ca^{2+} influx through the SOCs [8,23]. In general, TRPC1 is sensitive to Ca^{2+} store depletion and can be activated by STIM1, which is the sensor of the SOCs. As an SOCs component, TRPC1 can bind to STIM1 and ORAI to form a ternary complex that regulates SOCE [24]. Recent research has found that TRPC1 is involved extensively in vascular system development and functional maintenance. For example, Yu et al. found that silencing of the zebrafish *TRPC1* gene disrupted angiogenic sprouting of intersegmental vessels in zebrafish larvae. However, overexpression of TRPC1 prevented the angiogenic defect [25]. In addition, Yang et al. reported that knockdown of TRPC1 attenuates AngII-induced $[Ca^{2+}]_i$ and endothelial permeability [26]. Kumar et al. showed that a specific E3-targeted antibody to TRPC1 inhibited neointimal hyperplasia by suppressing SMC proliferation after vascular injury [11]. Further, Sweeney et al. discovered that a deficiency in TRPC1 inhibited pulmonary artery SMC proliferation and decreased capacitative Ca^{2+} entry [27]. Based on the importance of TRPC1 for vascular function, we focused on the role of TRPC1 in EPCs, which are important for repairing endothelial damage after vascular injury. Interestingly, our earlier work found that TRPC1-SOCs were involved in STIM1-induced Ca^{2+} influx in EPCs [12]. Moreover, in the present study, we demonstrated that downregulation of

TRPC1 by 2 different RNA silencing methods suppressed EPC proliferation and migration and decreased SOCE in vitro. In contrast, these effects were not observed in control cells, suggesting that TRPC1 is involved in the modulation of EPC proliferation, migration, and SOCE. In addition, it has been reported that intracellular Ca^{2+} is required for normal cell cycle progression, and upregulation of TRPC1 enhances cell cycle activity by increasing Ca^{2+} entry [11,28]. Accordingly, our data also indicate that TRPC1 silencing causes EPC cell cycle arrest in G1 phase by decreasing SOCE.

Finally, we have demonstrated that *Slfn1* is downstream of TRPC1 silencing-induced repression of EPC proliferation. *Slfn1*, a member of the *Slfn* gene family, has been reported to have antiproliferative activity by causing arrest in the G1 phase of the cell cycle in fibroblasts and thymocytes [18]. In the present study, the gene expression results from the Cell Cycle PCR gene chips showed that 9 genes were upregulated (*Ak1*, *Brca2*, *Camk2b*, *p21*, *Ddit3*, *Inha*, *Slfn1*, *Mdm2*, and *Prm1*) and 4 genes were downregulated (*Bcl2*, *Mki67*, *Pmp22*, and *Ppp2r3a*) more than 2-fold in the siRNA-TRPC1 group compared with the siRNA-control group. Interestingly, *Slfn1* was the most significantly upregulated gene in the microarray analysis, and real-time RT-PCR and western blot assays confirmed that *Slfn1* was upregulated about 9-fold in the siRNA-TRPC1 group compared with the siRNA-control group. Therefore, we hypothesize that *Slfn1* may be downstream of TRPC1. Further demonstrating this hypothesis, we used an *Slfn1*-blocking peptide to suppress *Slfn1* function in combination with TRPC1 silencing in EPCs. Surprisingly, we found that an *Slfn1*-blocking peptide reversed, at least in part, the abnormal EPC cell cycle distribution and proliferation induced by TRPC1 knockdown. Therefore, these results support the hypothesis that *Slfn1* is downstream of TRPC1. Other studies have found that *Slfn1* causes a cell cycle arrest by inhibiting the expression of cyclin D1 [29]. Whether *Slfn1* arrests the cell cycle in EPCs by suppressing cyclin D1 needs to be more extensively investigated. In addition, The 12 other genes that were upregulated or downregulated on the cell cycle gene chip array may be downstream of TRPC1 silencing. Further detailed functional investigations are needed to

TABLE 1. FOLD CHANGE IN THE EXPRESSION LEVEL OF CELL CYCLE GENES IN EPCs AFTER TRPC1 KNOCKDOWN

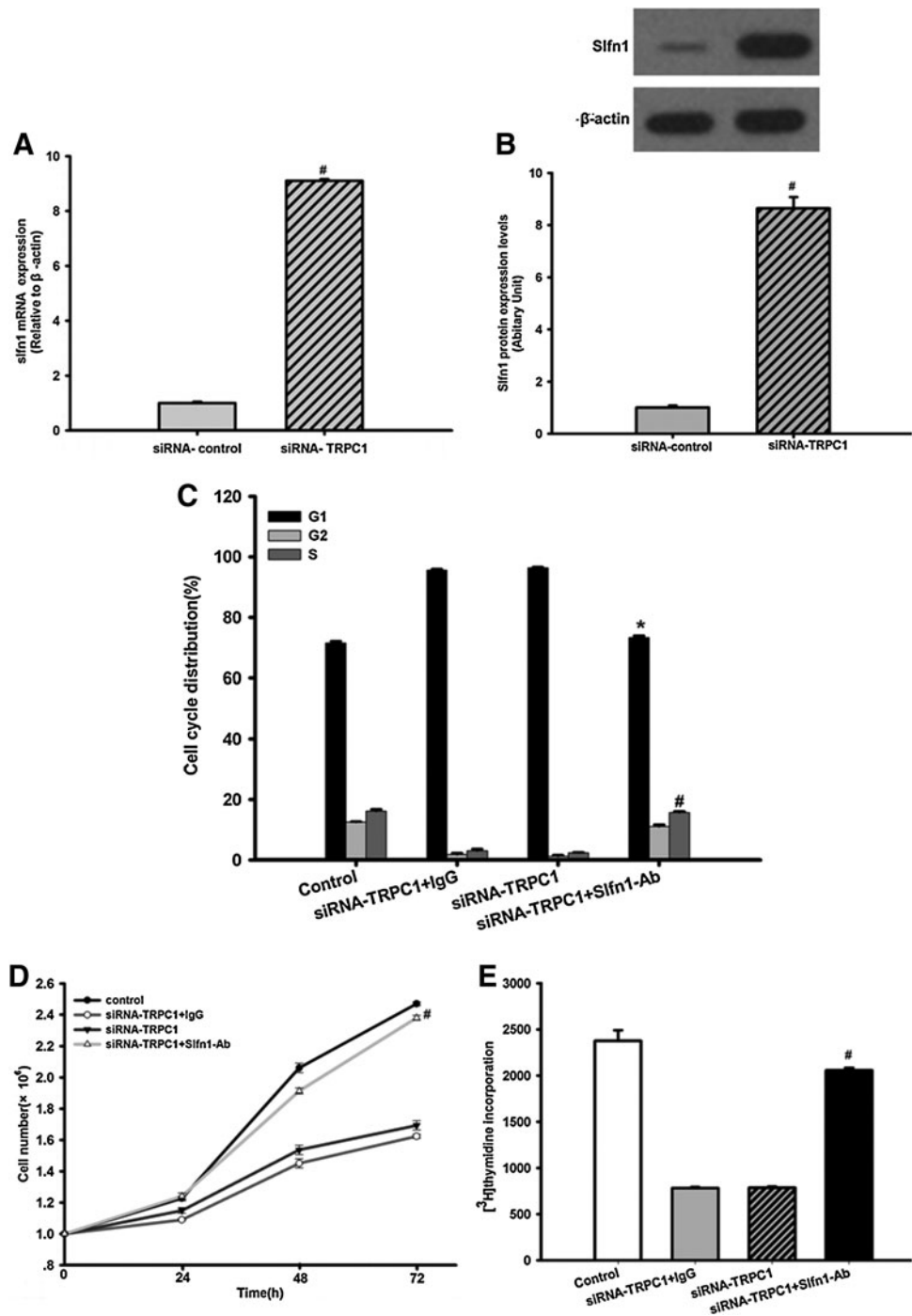
Symbol	GeneBank	Gene name	Fold change
Upregulated			
<i>Ak1</i>	NM_024349	Adenylate kinase 1	3.67
<i>Brca2</i>	NM_031542	Breast cancer 2	2.22
<i>Camk2b</i>	NM_021739	Calcium/calmodulin-dependent protein kinase II beta	3.23
<i>Cdkn1a</i>	NM_080782	Cyclin-dependent kinase inhibitor 1A (p21, Cip1)	3.44
<i>Ddit3</i>	NM_024134	DNA-damage inducible transcript 3	6.96
<i>Inha</i>	NM_012590	Inhibin alpha	5.52
<i>Slfn1</i>	XM_001068751	Schlafen 1	9.42
<i>Mdm2</i>	XM_235169	Mdm2 p53 binding protein homolog (mouse)	2.46
<i>Prm1</i>	NM_001002850	Protamine 1	3.02
Downregulated			
<i>Bcl2</i>	NM_016993	B-cell CLL/lymphoma 2	2.72
<i>Mki67</i>	XM_225460	Antigen identified by monoclonal antibody Ki-67	2.24
<i>Pmp22</i>	NM_017037	Peripheral myelin protein 22	2.27
<i>Ppp2r3a</i>	XM_576459	Protein phosphatase 2 (formerly 2A), regulatory subunit B'', alpha	2.99

Three separate experiments were performed in triplicate. $P < 0.05$ compared with siRNA-control.

FIG. 4. The impact of Slfn1 inhibition on the effects of TRPC1 knockdown in EPCs. **(A)** Slfn1 mRNA levels were determined using real-time RT-PCR. Transduction of EPCs with siRNA-TRPC1 clearly increased Slfn1 mRNA expression at 48 h post-transduction. $n=3$, $^{\#}P<0.05$ versus siRNA-control. **(B) Top:** Western blot analysis was used to evaluate Slfn1 protein levels. Equal loading was confirmed by staining of β -actin. Transduction of EPCs with siRNA-TRPC1 significantly increased Slfn1 protein expression after infection for 48 h ($n=3$). **Bottom:** Densitometric analysis of Slfn1 protein expression levels, normalized to expression levels of the housekeeping β -actin gene, was performed using the Quantity One program. Data represent the mean \pm SD from 3 different experiments. $n=3$, $^{\#}P<0.05$ versus siRNA-control.

(C) Impact of Slfn1 inhibition on cell cycle-related effects of TRPC1 knockdown in EPCs. Flow cytometry was used to determine the cell cycle distribution of EPCs transfected with siRNA-TRPC1, in the absence or presence of Slfn1-blocking peptide (Slfn1-Ab, 20 μ g/mL) or control goat IgG at 48 h post-transfection. Slfn1-blocking peptide increased the number of cells in S phase and decreased the number of cell in G1 phase, whereas a control antibody did not change the cell cycle distribution ($n=3$, $^{\#}P<0.05$ vs. siRNA-control S phase. $^*P<0.05$ vs. siRNA-control G1 phase). **(D)** EPC proliferation was clearly inhibited by siRNA-TRPC1, whereas Slfn1-blocking peptide partially reversed the effects of TRPC1 silencing. Data are presented as the mean \pm SD ($n=3$), $^{\#}P<0.05$ versus siRNA-TRPC1.

(E) [3 H]-thymidine incorporation was used to examine EPC proliferation. Transfection of EPCs with siRNA-TRPC1 significantly decreased the uptake of [3 H]-thymidine by EPCs 48 h after infection, whereas Slfn1-blocking peptide partly restored the effects of TRPC1 silencing. Data are presented as the mean \pm SEM from 3 different experiments, $n=9$, $^{\#}P<0.05$ versus siRNA-TRPC1. Slfn1, Schlafen 1.



clarify the role of these genes. We also noted that the EPCs function was impaired by cardiovascular risk factors such as elevated of C-reactive protein, increasing age and diabetic [30,31]. For one thing, C-reactive protein can attenuate the elevation of intracellular free calcium levels following stimulation with either platelet-activating factor or N-formyl-methionyl-leucyl-phenylalanine in guinea pig alveolar macrophages [32].

For another, TRPC1 expression is downregulated in the diabetic human vessels and old rat aorta [33,34]. Therefore, we speculate that the above cardiovascular risk factors may impair function of EPCs by TRPC1-Slfn1. However, further studies are needed to address this hypothesis.

In summary, our results provide evidence for the first time that TRPC1 is critical for the proliferation and migration of

EPCs and that Slfn1 is downstream of the TRPC1 knock-down effect on EPC proliferation. These findings provide a new mechanism for modulating the biological properties of EPCs and indicate that TRPC1 may be a new target for inducing vascular repair by EPCs.

Acknowledgments

Appreciation goes to Dr. Xiao-Qun Ye for his encouragement and kind help in this work. This study was supported in part by the National Natural Science Foundation of China (Grant 30770852, 81000070).

Author Disclosure Statement

No conflicts of interest exist.

References

- Landmesser U, B Hornig and H Drexler. (2004). Endothelial function: a critical determinant in atherosclerosis? *Circulation* 109:II27-II33.
- Ong AT, EP McFadden, E Regar, PP de Jaegere, RT van Domburg and PW Serruys. (2005). Late angiographic stent thrombosis (LAST) events with drug-eluting stents. *J Am Coll Cardiol* 45:2088-2092.
- Risau W. (1995). Differentiation of endothelium. *FASEB J* 9:926-933.
- Asahara T, T Murohara, A Sullivan, M Silver, R van der Zee, T Li, B Witzenbichler, G Schattman and JM Isner. (1997). Isolation of putative progenitor endothelial cells for angiogenesis. *Science* 275:964-967.
- Lewis RS. (2007). The molecular choreography of a store-operated calcium channel. *Nature* 446:284-287.
- Venkatachalam K, DB van Rossum, RL Patterson, HT Ma and DL Gill. (2002). The cellular and molecular basis of store-operated calcium entry. *Nat Cell Biol* 4:E263-E272.
- Yang M, A Gupta, SG Shlykov, R Corrigan, S Tsujimoto and BM Sanborn. (2002). Multiple Trp isoforms implicated in capacitative calcium entry are expressed in human pregnant myometrium and myometrial cells. *Biol Reprod* 67:988-994.
- Parekh AB and JW Putney, Jr. (2005). Store-operated calcium channels. *Physiol Rev* 85:757-810.
- Paria BC, SM Vogel, GU Ahmed, S Alamgir, J Shroff, AB Malik and C Tirupathi. (2004). Tumor necrosis factor- α -induced TRPC1 expression amplifies store-operated Ca^{2+} influx and endothelial permeability. *Am J Physiol Lung Cell Mol Physiol* 287:L1303-L1313.
- Bergdahl A, MF Gomez, AK Wihlborg, D Erlinge, A Eijolfsson, SZ Xu, DJ Beech, K Dreja and P Hellstrand. (2005). Plasticity of TRPC expression in arterial smooth muscle: correlation with store-operated Ca^{2+} entry. *Am J Physiol Cell Physiol* 288:C872-C880.
- Kumar B, K Dreja, SS Shah, A Cheong, SZ Xu, P Sukumar, J Naylor, A Forte, M Cipollaro, D McHugh, PA Kingston, AM Heagerty, CM Munsch, A Bergdahl, A Hultgardh-Nilsson, MF Gomez, KE Porter, P Hellstrand and DJ Beech. (2006). Upregulated TRPC1 channel in vascular injury *in vivo* and its role in human neointimal hyperplasia. *Circ Res* 98:557-563.
- Kuang CY, Y Yu, RW Guo, DH Qian, K Wang, MY Den, YK Shi and L Huang. (2010). Silencing stromal interaction molecule 1 by RNA interference inhibits the proliferation and migration of endothelial progenitor cells. *Biochem Biophys Res Commun* 398:315-320.
- Zhao X, L Huang, Y Yin, Y Fang, J Zhao and J Chen. (2008). Estrogen induces endothelial progenitor cells proliferation and migration by estrogen receptors and PI3K-dependent pathways. *Microvasc Res* 75:45-52.
- Huang PH, YH Chen, CH Wang, JS Chen, HY Tsai, FY Lin, WY Lo, TC Wu, M Sata, JW Chen and SJ Lin. (2009). Matrix metalloproteinase-9 is essential for ischemia-induced neovascularization by modulating bone marrow-derived endothelial progenitor cells. *Arterioscler Thromb Vasc Biol* 29:1179-1184.
- Gao P, DH Qian, W Li and L Huang. (2009). NPRA-mediated suppression of AngII-induced ROS production contribute to the antiproliferative effects of B-type natriuretic peptide in VSMC. *Mol Cell Biochem* 324:165-172.
- Guo RW, H Wang, P Gao, MQ Li, CY Zeng, Y Yu, JF Chen, MB Song, YK Shi and L Huang. (2009). An essential role for stromal interaction molecule 1 in neointima formation following arterial injury. *Cardiovasc Res* 81:660-668.
- Lu SY, DP Sontag, KA Detillieux and PA Cattini. (2008). FGF-16 is released from neonatal cardiac myocytes and alters growth-related signaling: a possible role in postnatal development. *Am J Physiol Cell Physiol* 294:C1242-C1249.
- Schwarz DA, CD Katayama and SM Hedrick. (1998). Schlafen, a new family of growth regulatory genes that affect thymocyte development. *Immunity* 9:657-668.
- Cosens DJ and A Manning. (1969). Abnormal electroretinogram from a *Drosophila* mutant. *Nature* 224:285-287.
- Humez S, G Legrand, F Vanden-Abeele, M Monet, P Marchetti, G Lepage, A Crepin, E Dewailly, F Wuytack and N Prevarskaya. (2004). Role of endoplasmic reticulum calcium content in prostate cancer cell growth regulation by IGF and TNF α . *J Cell Physiol* 201:201-213.
- Rao JN, O Platoshyn, VA Golovina, L Liu, T Zou, BS Marasa, DJ Turner, JX Yuan and JY Wang. (2006). TRPC1 functions as a store-operated Ca^{2+} channel in intestinal epithelial cells and regulates early mucosal restitution after wounding. *Am J Physiol Gastrointest Liver Physiol* 290:G782-G792.
- Louis M, N Zanou, M Van Schoor and P Gailly. (2008). TRPC1 regulates skeletal myoblast migration and differentiation. *J Cell Sci* 121:3951-3959.
- Pedersen SF, G Owsianik and B Nilius. (2005). TRP channels: an overview. *Cell Calcium* 38:233-252.
- Ong HL, KT Cheng, X Liu, BC Bandyopadhyay, BC Paria, J Soboloff, B Pani, Y Gwack, S Srikanth, BB Singh, DL Gill and IS Ambudkar. (2007). Dynamic assembly of TRPC1-STIM1-Orai1 ternary complex is involved in store-operated calcium influx. Evidence for similarities in store-operated and calcium release-activated calcium channel components. *J Biol Chem* 282:9105-9116.
- Yu PC, SY Gu, JW Bu and JL Du. (2010). TRPC1 is essential for *in vivo* angiogenesis in zebrafish. *Circ Res* 106:1221-1232.
- Yang LX, RW Guo, B Liu, XM Wang, F Qi, CM Guo, Yk Shi and H Wang. (2009). Role of TRPC1 and NF- κ B in mediating angiotensin II-induced Ca^{2+} entry and endothelial hyperpermeability. *Peptides* 30:1368-1373.
- Sweeney M, Y Yu, O Platoshyn, S Zhang, SS McDaniel and JX Yuan. (2002). Inhibition of endogenous TRP1 decreases capacitative Ca^{2+} entry and attenuates pulmonary artery smooth muscle cell proliferation. *Am J Physiol Lung Cell Mol Physiol* 283:L144-L155.
- Kahl CR and AR Means. (2003). Regulation of cell cycle progression by calcium/calmodulin-dependent pathways. *Endocr Rev* 24:719-736.

29. Brady G, L Boggan, A Bowie and LA O'Neill. (2005). Schlafen-1 causes a cell cycle arrest by inhibiting induction of cyclin D1. *J Biol Chem* 280:30723–30734.
30. Hill JM, G Zalos, JP Halcox, WH Schenke, MA Waclawiw, AA Quyyumi and T Finkel. (2003). Circulating endothelial progenitor cells, vascular function, and cardiovascular risk. *N Engl J Med* 348:593–600.
31. Turan RG, M Brehm, M Koestering, Z Tobias, T Bartsch, S Steiner, F Picard, P Ebner, CM Schannwell and BE Strauer. (2007). Factors influencing spontaneous mobilization of CD34+ and CD133+ progenitor cells after myocardial infarction. *Eur J Clin Invest* 37:842–851.
32. Foldes-Filep E, JG Filep and P Sirois. (1992). C-reactive protein inhibits intracellular calcium mobilization and superoxide production by guinea pig alveolar macrophages. *J Leukoc Biol* 51:13–18.
33. Erac Y, C Selli, B Kosova, KC Akcali and M Tosun. (2010). Expression levels of TRPC1 and TRPC6 ion channels are reciprocally altered in aging rat aorta: implications for age-related vasospastic disorders. *Age (Dordr)* 32:223–230.
34. Chung AW, K Au Yeung, E Chum, EB Okon and C van Breemen. (2009). Diabetes modulates capacitative calcium entry and expression of transient receptor potential canonical channels in human saphenous vein. *Eur J Pharmacol* 613:114–118.

Address correspondence to:

*Dr. Lan Huang
Institute of Cardiovascular Diseases of PLA
Xinqiao Hospital
Third Military Medical University
Chongqing 400037
People's Republic of China*

E-mail: xiaokcy@sina.com

Received for publication January 14, 2011

Accepted after revision March 1, 2011

Prepublished on Liebert Instant Online March 2, 2011